More than a Mutagenic Aflatoxin B1 Precursor: The Multiple Cellular Targets of Versicolorin a Revealed by Global Gene Expression Analysis

Carine Al-Ayoubi, Ophelie Rocher, Claire Nayles, Yannick Lippi, Julien Vignard, Sylvie Puel, Olivier Puel, Isabelle P. Oswald, Laura Soler

More than a mutagenic Aflatoxin B1 precursor: the multiple cellular targets of Versicolorin A revealed by global gene expression analysis

Carine Al-Ayoubi[a], Ophelie Rocher[a], Claire Naylies[a], Yannick Lippi[a], Julien Vignard[a], Sylvie Puel[a], Olivier Puel[a], Isabelle P Oswald[a], Laura Soler[a*]

[a] *Toxalim (Research Centre in Food Toxicology), Université de Toulouse, INRAE, ENVT, INP-Purpan, UPS, 31027, Toulouse, France*

[*] **Corresponding Author:**
Laura Soler
UMR 1331 TOXALIM, INRA/INP/UPS
Research Centre in Food Toxicology
180 chemin de Tournefeuille - BP.93173
F-31027 TOULOUSE cedex 3, France
Phone : +33 582 70 64 03
E-Mail : laura.soler-vasco@inrae.fr

Abstract

Versicolorin A (VerA), a precursor of the potent carcinogen aflatoxin B1 (AFB1), is an emerging mycotoxin. Recent research has highlighted the mutagenic and genotoxic properties of VerA, yet several facets of its pronounced toxicity remain unexplored. In the present study, we investigated early (6 h) transcriptomic changes induced by VerA in differentiated intestinal cells in non-cytotoxic conditions (1 and 3 µM) and compared its effects to those of AFB1 at 1 µM. Our findings indicated that VerA led to substantial alterations in global gene expression profiles, while AFB1 did not exhibit the same effect. As expected, both toxins caused alterations in gene expression associated with well-known aspects of their toxicity, including mutagenicity, genotoxicity, oxidative stress, and apoptosis. However, we also observed novel features of VerA toxicity, including the ability to cause mitochondrial dysfunction and to trigger a type-1 interferon response at least partially mediated by cGAS-STING. VerA also induced changes in the expression of genes involved in the regulation of cell shape and adhesion, transcription/translation as well as genes associated with tumor biology. Our results offer new evidence of the high toxicity of VerA and underscore the importance of further assessing the risk associated with its presence in food.

Keywords: Mycotoxins, Versicolorin A, Aflatoxin B1, transcriptome, intestine

Introduction

Aflatoxins, produced by toxigenic *Aspergillus* fungi, pose a significant global food safety threat (Bennett & Klich, 2003; Payros et al., 2021). These mycotoxins are widespread in hot and humid regions, contaminating various agricultural products such as cereals, nuts, seeds, and spices. Climate change projections indicate alarming increases in aflatoxin production in European maize crops (Bailly et al., 2018; Battilani et al., 2016). Among aflatoxins, aflatoxin B1 (AFB1) stands out as the most potent naturally occurring carcinogen (Schrenk et al., 2020). Its mode of action depends on its dihydrobisfuran structure, which is activated *in vivo* by cytochrome P450 enzymes and becomes a reactive mutagenic and genotoxic compound (Eaton et al., 2010; Smela et al., 2001). To address this threat, current global regulations concerning the presence of AFB1 in human food and animal feed authorize maximum levels of AFB1 ranging from 0.1 to 12 µg/kg depending on the product and its destination (European Communities, 2023).

The biosynthesis pathway of AFB1 is well known and involves the production of different bisfuranoid precursors that can accumulate in contaminated foodstuffs, including versicolorin A (VerA) (Caceres et al., 2020; Jiang et al., 2019). Like AFB1, VerA is synthesized by aflatoxigenic *Aspergillus* species. Additionally, non-aflatoxigenic *Aspergillus* species produce VerA, explaining its detection at higher concentrations than AFB1 in certain food products (Abdallah et al., 2017; Gauthier et al., 2020; Janić Hajnal et al., 2020). VerA is an emerging mycotoxin and some its toxicological characteristics have already been elucidated, but VerA is not yet subject to regulation. Like AFB1, VerA is highly mutagenic and genotoxic. Positive mutagenic responses have been demonstrated in bacterial mutation assays, when the effects were attributed to its metabolic activation in a potentially DNA-reactive form similar to that produced by AFB1 (Al-Ayoubi et al., 2022, 2023). Using metabolically competent and non-carcinogenic small intestinal cells (IPEC1) (Al-Ayoubi et al., 2023), we recently showed that a short (6 h) exposure to concentrations of VerA as low as 0.03 µM caused chromosomal damage and various pre-mutagenic lesions. Additional studies highlighted the greater complexity of VerA toxicity compared to that of AFB1, driven by certain key factors. For example, exposure to VerA induces higher levels of oxidative and replication stress in exposed cells than AFB1, which emerge as potentially important contributors to its genotoxicity, and are linked to the particular ability of VerA to induce DNA damage even in cells with poor metabolic activity (Gauthier et al., 2020; Theumer et al., 2018). In acellular models, VerA was also identified as a

potent inducer of mitochondrial respiration uncoupling, warranting more research (Kawai et al., 1983).

The present study aimed to understand the toxicity mechanisms of VerA in the intestine in order to improve our understanding of VerA toxicity, since present data suggest that VerA may have a more potent toxic effect than AFB1 and that the mechanisms underlying the toxicity of the two toxins are not the same.

2. Material and Methods

2.1. Toxins

VerA was produced using an in-house method detailed in (Theumer et al., 2018). VerA was isolated from an *Aspergillus parasiticus* strain (SRRC 0164) cultivated on wheat grain, followed by purification using Ultimate 3000 high-performance liquid chromatography (HPLC; Thermo Fisher Scientific, Courtaboeuf, France). The identity and purity of the VerA toxin were determined by HPLC with a diode array detector and a Zorbax C18 analytical column, with VerA peaks representing 97% of the signals (Theumer et al., 2018). AFB1 was purchased from Sigma. Both toxins were dissolved in DMSO (Sigma) at 10 mM and stored at -20 °C until further use.

2.2. Cell culture and exposure conditions

The non-tumorigenic and non-transformed intestinal cell line IPEC1 was chosen as a model due to its competence in terms of cytochrome P450 and p53 status which made these cells suitable for the study of aflatoxins and other pro-toxicants (Nossol et al., 2015). The IPEC1 cells were grown as described elsewhere (Al-Ayoubi et al., 2023). IPEC1 cells were differentiated into monolayers using Transwell devices prior as previously described (Al-Ayoubi et al., 2022) and exposed apically to 1 µM and 3 µM VerA, 1 µM AFB1, or to control solvent (DMSO) for 6 hours. As described previously (Al-Ayoubi et al., 2023), these conditions were not cytotoxic.

2.3. Microarray and functional analysis of differentially expressed genes

RNA isolation was performed as previously described (Pinton et al., 2010). Following extraction, the concentration and quality of the RNA were assessed using a Dropsense 96 UV/VIS droplet reader (Trinean, Belgium) and an Agilent 2100 Bioanalyzer (Agilent Technologies Inc., Santa Clara, CA, USA). The mean (± SD) RNA Integrity Number (RIN) was 9.53 ± 0.36. Gene expression profiling of the 16 samples (4 replicates per treatment group) were conducted at the GeT-TRiX platform (GénoToul, Génopole Toulouse Midi-Pyrénées) using Agilent Sureprint G3 Porcinet 60K_DEC2011 microarrays (8 × 60K, design 037880) in accordance with the manufacturer's instructions, as described in (Pierron et al., 2022). Microarray data and experimental details are available in NCBI's Gene Expression Omnibus (Edgar et al., 2002) and are accessible through GEO Series accession number GSE267572 (https://www.ncbi.nlm.nih.gov/geo/query/acc.cgi?acc=GSE267572).

2.4. Real-time Quantitative PCR (RT-qPCR) analysis

RT-qPCR assays were performed as described elsewhere (Hasuda et al., 2022). Primers (Table S1, Supplementary data) were designed using PrimerQuest software (Integrated DNA Technologies, San Diego, CA, USA) and were obtained from Sigma-Aldrich. Data analyses were performed with the LinRegPCR freeware (version 2016) and normalized against different reference genes (*HMBS, HPRT, TOP2B*).

2.5. Protein Extraction and Immunoblotting

Total protein extraction and immunoblotting were performed using methods detailed elsewhere (Soler et al., 2020) using the primary antibodies listed in Table S2 and species-specific fluorescent secondary antibodies (Biotium, Inc., Fremont, CA, USA). Target proteins were visualized using a Fluorescent Imaging Scanner (Azure Biosystems, Dublin, CA, USA) and the resulting images were digitized and quantified using Image Studio Lite Software v5.2 (Li-Cor Biosciences, Lincoln, NE, USA). Band intensity values in each lane were normalized to their respective total protein staining, which was performed using SYPRO™ Ruby protein blot stain (Thermo Fisher Scientific) after transfer using ChemidDoc (SYPRO™ Ruby-stained membranes; Bio-Rad).

2.6. Evaluation of sirtuin activity in subcellular fractions

Sirtuin deacetylase activity was assessed using a single reagent luminescence-based assay (SIRT-Glo^{TM}, Promega). Protein extraction and subcellular fractionation (cytoplasmic and nuclear protein fractions) were obtained using a commercially available kit (Subcellular Protein Fractionation Kit, Thermo Scientific). NAD^+ dependent histone deacetylase activity was then measured in the presence of a histone deacetylase (HDAC) inhibitor, Trichostatin A (1 µg/mL, Sigma), following the manufacturer's instructions using a luminescence plate reader (TECAN Spark, Männedorf, Switzerland).

2.7. Evaluation of mitochondrial dysfunction

The impact of VerA on mitochondria was evaluated by comparing the ability of exposed cells to produce ATP under non-cytotoxic conditions, both in the presence of glucose and when glucose was replaced by D-galactose. Briefly, 10^4 cells per well were seeded in white 96-well

plates and exposed to 1 µM and 3 µM VerA, for 6 h in the presence and absence of glucose, which was subsequently replaced by D-galactose (Sigma).

The analysis was completed by evaluating cytotoxicity and caspase 3/7 activation using the CytoToxFluor™ fluorescent assay (CytoTox-Fluor™, Promega) and the Caspase-Glo® 3/7 luminescent assay (Caspase-Glo, Promega), respectively. Following the manufacturer's instructions, the assays were performed in cells (5.10^3 cells/well) seeded in white 96-well plates and exposed to the aforementioned concentrations of VerA for 6 hours.

The luminescence and fluorescence signals were recorded after exposure with a multimode microplate reader (TECAN Spark). Three independent experiments with three technical replicates were conducted for each condition to ensure the reliability of the results.

2.8. Statistical analysis

Microarray data were analyzed using R (R Core Team, 2018) and Bioconductor packages (Huber et al. 2015) as described in GEO accession GSE267572. Raw data (median signal intensity) were filtered, log2 transformed and normalized using the quantile method (Bolstad et al., 2003). A model was fitted using the limma lmFit function (Ritchie et al., 2015). Pair-wise comparisons between biological conditions were applied using specific contrasts. A correction for multiple testing was applied using the Benjamini-Hochberg procedure (BH, Benjamini & Hochberg, 1995) to control the false discovery rate (FDR). Probes with FDR < 5% were considered to be differentially expressed between conditions. The results were explored using MATRIX APP (Lippi & Soubès, 2023, https://matrix.toulouse.inrae.fr/). Hierarchical clustering was applied to the samples and the differentially expressed probes using 1-Pearson correlation coefficient as distance and Ward's criterion for agglomeration and the results are illustrated as a heat map. Functional analysis of the differentially expressed genes lists was performed using the EnrichR web server (Chen et al., 2013; Kuleshov et al., 2016; Xie et al., 2021) and Ingenuity Pathway Analysis tool (QIAGEN, Valencia, CA, USA). Only pathways with a P value < 0.05 are shown here.

For cell-based assays, data from qPCR and immunoblotting tests are expressed as mean ± standard deviation (SD) of three independent experiments. The statistical analysis was performed by a one-way Anova followed by Bonferroni's multiple comparisons tests using

GraphPad Prism version 9.0.2 (San Diego, California USA). A p-value < 0.05 was considered statistically significant.

3. Results and discussion

3.1 VerA, but not AFB1, induces marked changes in the gene expression profiles of differentiated intestinal epithelial cells

Exposure of intestinal cells to these conditions resulted in significant changes (FDR < 0.05; fold-change > 1) in gene expression compared to vehicle (DMSO) controls. AFB1 induced changes in 79 genes, while 1 µM VerA and 3 µM VerA induced changes in 3,261 and 5,211 genes, respectively (Fig. 1, A). Microarray results were confirmed by RT-qPCR analysis using selected genes (*FLVCR2*, *SRM*, *MAPK2K6*, *SERPINB2* and *MX2*), and gene expression results obtained using the two techniques were in agreement (Table S3). Our study found that AFB1 exposure had a low impact on the transcriptome of intestinal cells, in contrast to the high impact of VerA. This observation aligns with previous research conducted on proliferating epithelial intestinal Caco-2 cells (Gauthier et al., 2020). However, it's important to note that our study identified fewer genes affected by VerA and AFB1 exposure compared to the aforementioned study. This discrepancy may be attributed to the non-proliferative state of the monolayer cells, as previously described for another mycotoxin (Hinze & Boucrot, 2018; Luo et al., 2021).

Principal component analysis (PCA) revealed that the concentration of VerA was the main source of variance (Fig. 1, B). The Venn diagram in Figure 1A reveals significant similarity in VerA-treated samples. Specifically, 2,788 genes were identified in samples treated with both 3 µM and 1 µM VerA, accounting for 85.5% of all genes regulated at a VerA concentration of 1 µM. Additionally, 65 genes were found in both AFB1- and VerA-treated samples (at concentrations of both 3 µM and 1 µM), representing 82.3% of all genes regulated at an AFB1 concentration of 1 µM.

Next, double hierarchical clustering was performed to identify specific and shared expression profiles for differentially expressed probes (FRD < 5%) identified in response to treatments. The results are presented in the form of a heatmap (Fig. 1C). Three distinct gene clusters are highlighted as alternative grey levels next to the dendrogram on the left based on the relationships between their expression (Fig. 1 D). Cluster 1 included 2,695 genes that were down-regulated in all VerA-treated cells compared to in controls, although AFB1 had relatively

weaker effects and the responses to VerA were dose dependent. Functional analysis (Table S4) revealed that the main regulated pathways of this cluster (i.e. those showing the most significant enrichment) were related to cadherin-mediated cell adhesion and changes in shape and their related signaling, as well as RNA processing. The predicted upstream regulators of the genes in this cluster were mainly *TP53* and *TGFB1*. The 'top tox' list (set of molecules that are known to be involved in a particular type of toxicity) was primarily related to cell death. Notably, the list of 'top analysis-ready molecules' (an output list showing the genes with the strongest regulation; Table S5) mainly included genes involved in regulating cell adhesion and shape-related functions (*DKK1*, *SPRED1*, *TUBB6*, *FGD6*), and p53-related signaling (*PPP1RI3B*, *PRRG1*, *NAV1*).

Cluster 2 consisted of 726 genes that were upregulated at a similar magnitude in all treated cells. The differentially expressed genes in this cluster were mainly related to interferon signaling, methionine and L-cysteine degradation, mesenchymal cell differentiation mediated by RUNX1 and caspase activation (Table S6). The primarily predicted upstream regulators of these processes were identified as poly rI:rC RNA and RNASEH2A. In the context of toxicity, the 'top tox' molecular set was primarily associated with oxidative stress. The genes that showed the strongest regulation in cluster 2 (Table S7) included several involved in processes related to tumorigenesis (*TGFA*, *RDH16*, *UTRN*), transcription regulation (*KLF3*), DNA repair (*AHDC1*) and apoptosis (*CASP5*).

Cluster 3 included 1,997 genes upregulated in all treated samples compared to in the control group but the magnitude of change in gene expression was only high in cells treated with VerA, mostly at a concentration of 3 μM. Functional analysis based on the most significant p-values, revealed that the main enriched pathways in this dataset were the sirtuin signaling pathway, mitochondrial dysfunction, interferon signaling, and processes related to DNA damage and repair (Table S8). *TP53* and *HNF4A* were identified as main predicted upstream regulator in many of these processes. Additionally, the enriched GO molecular functions mainly included oxidized DNA binding and glutathione transferase activity. The genes showing the strongest regulation in cluster 3 (Table S9) are mainly known for their critical functions in tumor biology (*NR3C2*, *SNTB1*, *ABLIM1*, *PPP1R9A*, *MBP* and *GHR*). The list was completed by chaperones and genes involved in immune signaling (*CCDC30*, *FLVCR2* and *SLC7A7*).

3.2 Both AFB1 and VerA induce overexpression of DNA damage response-related genes: mutagenicity as a common mechanism of action

Almost all the genes significantly regulated by AFB1 were also regulated by VerA at both concentrations tested (65 genes; Fig.1, A) although the fold-changes in gene expression were more pronounced at a concentration of 3 µM VerA than at 1 µM VerA and that of AFB1 for these genes in all functional categories. The main function of these genes was shown to be associated with DNA repair, cell cycle control and apoptosis. This result reflects the common toxicity of AFB1 and VerA as genotoxins. In our previous works, we demonstrated that VerA is likely to be biotransformed into a mutagenic derivative, which is known to be the main mechanism of action of AFB1 (Al-Ayoubi et al., 2022). Indeed, the signaling pathway 'diseases of mismatched repair' that is known to be activated in the presence of mutagenic agents, is overrepresented in our dataset. Further, both toxins can cause oxidative DNA damage (Al-Ayoubi et al., 2023). Our gene expression results consequently reflect the fact that both toxins can activate a DNA damage response (DDR) triggered by their mutagenicity.

According to our data, the DDR induced by both toxins seems to be mediated by ataxia telangiectasia-mutated - breast cancer 1 (ATM-BRCA1) and the tumor suppressor protein p53 pathways, potentially involving upstream regulators with roles already described during the cell response to AFB1, such as p53, HNF-4 α (Marrone et al., 2016) and RNase H2. In response to DNA damage, p53 binds DNA and mediates transcriptional activation of genes whose products trigger cell-cycle arrest, DNA repair and/or apoptosis (Riley et al., 2008). The essential role of this tumor suppressor protein in the alleviation of the toxicity of AFB1 is known, and a mutation in codon 249 of the *TP53* gene is tightly linked with the development of hepatocarcinoma in individuals exposed to AFB1 (Hussain et al., 2007). While previous studies suggested that p53 is not essential for cell cycle control and apoptosis induction in intestinal cells exposed to VerA (Gauthier et al., 2020), we observed that 53BP1 is an important mediator of VerA-induced DDR, as it is recruited in IPEC1 cells exposed to VerA (Al-Ayoubi et al., 2023). According to the literature, some post-translational modifications are important regulators of p53 activity (Meek & Anderson, 2009) for example, Ser15 phosphorylation and Lys382 acetylation. Previous studies showed that AFB1 induces significantly higher levels of p53-Ser15 phosphorylation than VerA in Caco-2 and HepG2 cells (Budin et al., 2021; Gauthier et al.,

2020), whereas in our study, only VerA induced a significant increase of Ser15-phosphorylated p53 levels in IPEC1 cells (at the highest concentration), while AFB1 did not (Fig. 2). What is more, only VerA induced changes in gene expression in many p53-responsive genes including *PPP1RI3B*, *PRRG1*, *NAV1, CD82*, *PIK3R3*, *PIK3C2B* and *SESN1*, suggesting that VerA activates p53 responses in exposed IPEC1 cells. Indeed, our results agree with previous findings indicating that wild-type p53 dynamics varies substantially between cell lines (Stewart-Ornstein & Lahav, 2017).

In addition to phosphorylation, Lys382 acetylation is a p53 transactivation pathway that enhances the sequence-specific DNA-binding activity of p53 in response to DNA damage, and is controlled by several NAD^+-dependent deacetylases, including sirtuin 1 (SIRT1). Interestingly, we observed significant overrepresentation of the sirtuin signaling pathway and, in general, of genes exhibiting deacetylase activity in VerA-exposed cells. We examined the cytoplasmic and nuclear sirtuin-dependent deacetylase activity in IPEC1 cells exposed to 3 μM VerA and only detected a significant increase in nuclear sirtuin-dependent deacetylase activity (Fig. 3, A). Protein abundance levels of the nuclear sirtuin SIRT1 (Fig 3, B) were also significantly increased in the presence of VerA (at both 3 μM and 1 μM), as well as in the presence of AFB1 (1 μM). In parallel with these results, we observed a concomitant VerA-dependent regulation of the expression of downstream genes within the SIRT1 pathway, such as *PPARGC-1*, *PPARG* and *FXR* (p-value < 0.05). These data suggest that sirtuins, particularly SIRT1, play a role in the toxicity of VerA. Since SIRT1 mediates the acetylation of p53 and this posttranslational modification is important for the activity of p53 (Ren et al., 2019), we investigated whether VerA induces changes in Lys382-acetylation of p53. However, our findings revealed a non-significant accumulation of acetylated p53 in exposed cells (Fig. 2). More research is thus needed to understand the role of SIRT1 in VerA toxicity, which may involve transcriptional regulation of p53/histone acetylation (Zhang & Kraus, 2010), or be associated with mitochondrial toxicity (discussed below) and apoptosis induction (Tang, 2016).

Our results confirm that DDR is initiated by both AFB1 and VerA, confirming a common mechanism of action in these structurally related compounds, based on their mutagenicity. While this requires further studies, our data also suggest that, contrary to previously published results, p53 may be also an important mediator of DDR for VerA, as it is for AFB1.

3.3 VerA: an inhibitor of transcription?

Previous results indicated that VerA genotoxicity involves more mechanisms than that of AFB1, mainly the induction of a higher level of replication stress (Al-Ayoubi et al., 2023; Gauthier et al., 2020). Replication stress may explain the ability of VerA to induce genotoxicity in cell lines that lack metabolic activity, in contrast to AFB1 (Theumer et al., 2018). The results of functional analysis of our data are in line with this hypothesis and provide additional clues to how VerA could induce replication stress. We found an enrichment of molecular functions related to the biology of DNA and RNA in VerA-regulated genes. The RNA metabolism pathway, along with molecular functions related to RNA and snoRNA binding were significantly overrepresented. When we extracted the list of genes associated with the GO "RNA binding" from our dataset (Table 1), we observed that the expression of these genes is only regulated by VerA. Most of these genes, which are essential for correct transcription and translation, were significantly down-regulated, while the expression of the topoisomerases 1 and 2A was significantly up-regulated. Previous results (Gauthier et al., 2020) indicated that VerA exposure leads to the significant accumulation of small nucleolar H/ACA RNA (SNORA) and C/D box RNA (SNORD) genes. Taken together, these results suggest that VerA may disrupt DNA/RNA biology, which at least partially explains the known activation of an early ATR response, increased FANCD2 nuclear accumulation and the overall high replication stress induced by VerA (Al-Ayoubi et al., 2023; Gauthier et al., 2020). Additional studies are needed to understand the mechanism by which VerA interferes with transcription and/or translation.

3.4 VerA induces higher oxidative stress than AFB1 depending on changes in gene expression

Oxidative stress was one of the 'top tox' to emerge from our functional analysis of genes in cluster 2, while oxidized DNA binding was identified as an enriched molecular function of genes in cluster 3. Additionally, two overrepresented pathways in cluster 2 were associated with enhanced degradation of methionine and its intermediary metabolite, L-cysteine. Since methionine plays a significant role as a scavenger of reactive oxygen species (ROS) (Shen Luo

& Levine, 2009), our results suggest toxin-mediated oxidative stress and, as a consequence, enhancement of methionine degradation. Oxidative stress occurs in AFB1-exposed cells as a consequence of ROS accumulation during the biotransformation of AFB1 into its reactive epoxide form (Kozieł et al., 2021). This leads to activation of the antioxidant Nrf2/ARE pathway and depletion of the methionine cell pool. It is known that dietary methionine supplementation mitigates the toxicity of AFB1 by modulating an Nfr2- mediated antioxidant pathway (Elwan et al., 2021). To check whether the predicted increased degradation of methionine was associated with changes in the expression of effector genes in the Nrf2 response (Table 2), we monitored expression of key genes in our dataset. Our analysis revealed that exposure to VerA was significantly associated with upregulation of *CAT*, *GPX8*, *NQO1* and *GCLM* and with downregulation of *SOD2*, *GPX2*, *HMOX1*, *GCLC* and *TXN*. In contrast, exposure to AFB1 only caused significant downregulation of the intestinal glutathione peroxidase *GPX2*. These results suggest the presence of oxidative stress and the activation of Nrf2 responses in VerA- but not in AFB1-treated cells. This is in line with the results of previous studies showing that VerA induces higher oxidative stress than AFB1 in intestinal cells, characterized by a significant accumulation of ROS, including hydrogen peroxide and superoxide anion (Gauthier et al., 2020).

3.5 VerA, but not AFB1, induces mitochondrial toxicity and an IFN-I response mediated, at least partly, by cGAS-STING

Functional analysis indicated an increase in oxidoreductase activity and signs of mitochondrial dysfunction, particularly among the genes in cluster 3. Only VerA, mainly at the highest concentration, but not AFB1, regulated these genes associated with the mitochondrial dysfunction, as identified by the functional analysis. We observed that, among the genes regulated across all mitochondrial respiratory complexes, those in complex IV underwent a more pronounced change in their fold-change ratio (Fig. S1). These data suggest that VerA is toxic to the mitochondria, which was already suggested in early studies using acellular models (Kawai et al., 1983). In fact, mycotoxins with a hydroxyl group at the β-position of their anthraquinone nucleus, like VerA, are known to have a strong uncoupling activity in mitochondrial respiration (Kawai et al., 1983), which is responsible for their high cytotoxicity.

Reversal potential analysis, using planar lipid bilayer membranes, showed that VerA facilitates proton permeability and increases conductance, which partly explain its uncoupling effect on mitochondrial respiration (Muto et al., 1997).

The mitotoxicity of VerA was confirmed in our cell model since a significant drop in ATP levels was observed when exposed IPEC1 cells were forced to only use oxidative phosphorylation to produce ATP. This effect was associated with significant activation of caspase 3/7, effectors of the intrinsic apoptotic pathway. Although cytotoxicity did not increase significantly, cells exposed to 3 μM VerA showed more pronounced mitotoxicity and oxidative and pro-apoptotic processes than cells exposed to 1 μM VerA (Fig. 4). Moreover, VerA (but not AFB1) promoted changes in genes related with mitophagy such as *SQSTM1* and *HSPD1*. HIF-1, a protein known to respond to mitochondrial stress (Huang et al., 2023), accumulated in cells exposed to VerA, while BNIP3L, a protein degraded together with mitochondria during mitophagy, was significantly depleted (Fig. S3). All these findings provide strong evidence that VerA has mitotoxic properties, calling for characterization of its impact on cell respiration, metabolism and mitochondrial biogenesis.

While we cannot rule out involvement of ATM-dependent NFκB activation in response to genomic DNA damage, the modulation of genes associated with activation of interferon (IFN) signaling responses observed in our dataset (Table S10) may also be attributed to VerA-specific mitochondrial dysfunction. Indeed, exposure to VerA induced the over-expression of IFN-β1, the IFN receptor IFNGR2, the transcriptional regulators of type I IFN-dependent immune responses, and the interferon-inducible gene *IRF3* as well as the IFN-inducible genes *GBP2*, *MX2*, *OAS1* and *OAS2*. The interferon-I pathway can be activated by the accumulation of ROS and mitochondrial ROS (MitoSOX) during mitochondrial toxicity. As mentioned earlier, VerA is known to induce significantly higher oxidative stress than AFB1 (Gauthier et al., 2020), and exposure to 3 μM VerA was able to increase the levels of mitochondrial superoxide in IPEC1 cells after 24 hours of incubation (Fig. 4, E). In addition, mitochondrial damage can lead to the release of mitochondrial DNA (mtDNA) in the cytoplasm, which is sensed by the cyclic GMP–AMP synthase-stimulator of interferon response cGAMP interactor 1 (cGAS-STING) pathway, a potent inducer of type I IFN responses (West et al., 2015). Our data strongly suggest that cGAS-STING is activated upon exposure to VerA, as we observed significant upregulation of STING, as well as the effector genes of this pathway *TBK1*, *PTEN*, *PIAS1* and *STAT1/2* (Table S10). Along with these changes, cells exposed to VerA also accumulated significant quantities

of phospho-STAT1 (Fig. S3). In line with these findings, our study indicates that similar pro-inflammatory signaling pathways engaged by mtDNA include the NLRP3 inflammasome and NF-κB pathways following exposure to VerA. Signs of activation of both pathways by VerA were observed, such as higher gene expression of CASP1 and IL1B (Table S10), as well as accumulation of IKBα protein in exposed cells (Fig. S3). Overall, VerA is toxic to mitochondria, inducing a cascade of pro-inflammatory signals, which highlights the importance of understanding the relevance of these events, as mtDNA-induced responses are implicated in the promotion of autoimmune, metabolic and degenerative diseases.

3.6 Is VerA cancerogenic? Evidence from gene expression analysis

As discussed above, VerA is mutagenic and genotoxic, and shares some features of toxicity with AFB1. Yet, while AFB1 is known to be a cancerogenic compound, this is not the case for VerA. However, the present dataset has provided information concerning the phenotypic changes that cells undergo after exposure to VerA that suggest a cancerogenic potential.

A group of genes in cluster 1 is functionally involved in the remodeling of epithelial adherent junctions, integrin signaling, and actin cytoskeleton signaling. These genes were significantly downregulated (adjusted $p<0.05$) in cells exposed to VerA in a concentration-dependent manner, but not in cells exposed to AFB1 (Table S5, Fig.S2). These changes in gene expression suggest that epithelial cells exposed to VerA undergo phenotypical changes related to loss of adhesion, alterations to cell shape and to cell junctions. Functional analysis predicted that the upstream regulators of these changes would transform growth factor-beta (TGF-β; TableS4) and tumor protein p53 (*TP53*; Table S4). TGF-β is a potent growth suppressor of epithelial cells and mediates cell differentiation of intestinal epithelial cells (Morikawa et al., 2016), and the mutation of *TP53* has been associated with, among other things, increased adhesion ability (Lee et al., 2015). In line with these findings, many genes in this cluster were found to be involved in cell growth, death control and motility (Table S5). The 10 top most regulated genes in this cluster code for proteins present in the cytoskeleton (*TUBB6*, *FDG6*), nucleosome (*PROB1*) or chaperone protein complexes (*SDF2L1*) or are else involved in p53 signaling (*PPP1R13B*, *PRRG1*, *NAV1*, *EEPD1*) or in the regulation of epithelial-mesenchymal transition (EMT) initiation (*DKK1*, *SPRED1*). In line with these results, genes related to RUNX1-mediated signaling (RUNX1 regulates TGF-β induced EMT; (Lu et al., 2020)) were overrepresented in cluster 2, and many genes involved in EMT initiation and progression, such as *TGFA, SNTB1, ABLIM* and *PPP1R9A,* were among the most regulated genes in clusters 2 and 3. EMT is a

process in which polarized epithelial cells lose their epithelial phenotype and adopt a mesenchymal cell phenotype, including, among other changes, increased resistance to apoptosis, which is often associated with malignant transformation of epithelial cells (Koen & Collier, 2009).

Despite all the evidence for the induction of an EMT in differentiated intestinal cells in our dataset, we were not able to confirm modulation of CTNNβ and E-cadherin at the protein level. Furthermore, the abundance of other proteins, including the actin-regulating protein cofilin and the mesenchymal phenotype marker vimentin, did not change (Fig. S3). Because the short exposure time (6 h) may be insufficient to induce transition to a mesenchymal phenotype, studies with adjusted exposure conditions (non-cytotoxic concentrations, longer exposure) are now needed to determine whether VerA reduces the presence of membrane E-cadherin, causes trans-nucleation of β-catenin or promotes changes in the actin cytoskeleton related to an EMT transition, plus to identify the role of TGF-β in this phenomenon.

Interestingly, several of the genes most regulated by VerA were shown to be involved in tumor biology. The list includes different tumor suppressing genes such as *RDH16*, strongly regulated in hepatocellular cancer (Zhu et al., 2020), *UTRN*, which is mutated in a number of tumors (Y. Li et al., 2007) and *NFIB*, also known to have tumor suppressive functions in many malignancies. Other genes known to be involved in colorectal tumorigenesis such as *NR3C2*, which is reported to function as a tumor suppressor (J. Li & Xu, 2022), *GHR,* which is frequently expressed in human colorectal cancers (Yang et al., 2004) and *ABLIM1*, which promotes growth and metastasis of colorectal cancer (He et al., 2024), were all modulated. This list is completed by *SNTB1*, which plays a crucial role in the stemness maintenance of cancer cells (Liang et al., 2021) and *PPP1R9A*, an imprinted gene, whose imprinting loss is linked with the development of different epithelial types of cancer (Hsu et al., 2016).

Overall, our results support the hypothesis that exposure to VerA is associated with the induction of cell malignancy in intestinal cells, underlining the importance of investigating the carcinogenic capacities of VerA.

4. Conclusion

Our study reveals new insights into VerA toxicity, confirming its greater toxicity to intestinal cells compared to AFB1. While VerA-induced transcriptome changes mirror those associated with DNA damage response, oxidative stress, and apoptosis seen with AFB1, VerA affects a

larger number of genes and exhibits unique toxic aspects. Our data suggest that VerA's genotoxicity may involve replication stress due to RNA/DNA biology disruption. Additionally, VerA shows mitotoxicity in intestinal cells, potentially linked to interferon-I immune responses and inflammatory cascades. Dysregulation of genes related to a carcinogenic cell phenotype was also observed. These findings contribute valuable toxicity data for assessing VerA exposure risk.

Acknowledgments

This research was supported in part by the ANR grants "Versitox" (ANR-18-CE21-0009), "Precursors" (ANR-23-CE34-017) and the INRAE-SA project "VersiTrans". The authors would like to thank Daphne Goodfellow for English editing.

5. References

Abdallah, M. F., Girgin, G., Baydar, T., Krska, R., & Sulyok, M. (2017). Occurrence of multiple mycotoxins and other fungal metabolites in animal feed and maize samples from Egypt using LC-MS/MS. Journal of the Science of Food and Agriculture, 97(13), 4419–4428. https://doi.org/10.1002/jsfa.8293

Al-Ayoubi, C., Alonso-Jauregui, M., Azqueta, A., Vignard, J., Mirey, G., Rocher, O., Puel, O., Oswald, I. P., Vettorazzi, A., & Soler, L. (2023). Mutagenicity and genotoxicity assessment of the emerging mycotoxin Versicolorin A, an Aflatoxin B1 precursor. Environmental Pollution, 335, 122276. https://doi.org/10.1016/j.envpol.2023.122276

Al-Ayoubi, C., Oules, J., Person, E., Bruel, S., Bouville, A., Pinton, P., Oswald, I. P., Jamin, E. L., Puel, O., & Soler, L. (2022). Metabolism of versicolorin A , a genotoxic precursor of aflatoxin B1 : Characterization of metabolites using in vitro production of standards. Food and Chemical Toxicology, 167(June), 113272. https://doi.org/10.1016/j.fct.2022.113272

Bailly, S., Mahgubi, A., Carvajal-Campos, A., Lorber, S., Puel, O., Oswald, I., Bailly, J.-D., & Orlando, B. (2018). Occurrence and Identification of *Aspergillus* Section *Flavi* in the Context of the Emergence of Aflatoxins in French Maize. Toxins, 10(12), 525. https://doi.org/10.3390/toxins10120525

Battilani, P., Toscano, P., Van Der Fels-Klerx, H. J., Moretti, A., Camardo Leggieri, M., Brera, C., Rortais, A., Goumperis, T., & Robinson, T. (2016). Aflatoxin B 1 contamination in maize in Europe increases due to climate change. Scientific Reports, 6, 1–7. https://doi.org/10.1038/srep24328

Benjamini, Y., & Hochberg, Y. (1995). Controlling the False Discovery Rate: A Practical and Powerful Approach to Multiple Testing. Journal of the Royal Statistical Society: Series B (Methodological), 57(1), 289–300. https://doi.org/10.1111/j.2517-6161.1995.tb02031.x

Bennett, J. W., & Klich, M. (2003). Mycotoxins. Clinical Microbiology Reviews, 16(3), 497–516. https://doi.org/10.1128/CMR.16.3.497-516.2003

Bolstad, B. M., Irizarry, R. A., Astrand, M., & Speed, T. P. (2003). A Comparison of Normalization Methods for High Density Oligonucleotide Array Data Based on Variance and Bias. Bioinformatics, 19(2), 185–193. https://doi.org/10.1093/bioinformatics/19.2.185

Budin, C., Man, H. Y., Al-Ayoubi, C., Puel, S., van Vugt-Lussenburg, B. M. A., Brouwer, A., Oswald, I. P., van der Burg, B., & Soler, L. (2021). Versicolorin A enhances the genotoxicity of aflatoxin B1 in human liver cells by inducing the transactivation of the Ah-receptor. Food and Chemical Toxicology, 153, 112258. https://doi.org/10.1016/j.fct.2021.112258

Caceres, I., Al Khoury, A., El Khoury, R., Lorber, S., P. Oswald, I., El Khoury, A., Atoui, A., Puel, O., & Bailly, J.-D. (2020). Aflatoxin Biosynthesis and Genetic Regulation: A Review. Toxins, 12(3), 150. https://doi.org/10.3390/toxins12030150

Chen, E. Y., Tan, C. M., Kou, Y., Duan, Q., Wang, Z., Meirelles, G. V., Clark, N. R., & Ma'ayan, A. (2013). Enrichr: Interactive and collaborative HTML5 gene list enrichment analysis tool. BMC Bioinformatics, 14, 128. https://doi.org/10.1186/1471-2105-14-128

Eaton, D. L., Beima, K. M., Bammler, T. K., Riley, R. T., & Voss, K. A. (2010). Hepatotoxic Mycotoxins. Comprehensive Toxicology, 9, 527–569.

Elwan, H., Xie, C., Miao, L. P., Dong, X., Zou, X., Mohany, M., Ahmed, M. M., Al-Rejaie, S. S., & Elnesr, S. S. (2021). Methionine alleviates aflatoxin B1-induced broiler chicks embryotoxicity through inhibition of caspase-dependent apoptosis and enhancement of cellular antioxidant status. Poultry Science, 100(8), 101103. https://doi.org/10.1016/j.psj.2021.101103

European Communities. (2023). Commission Regulation (EU) 2023/915 of 25 April 2023 on maximum levels for certain contaminants in food and repealing Regulation (EC) No 1881/2006 (Text with EEA relevance). Official Journal of the European Union, L119(Document L:2023:119:TOC), 103–157.

Gauthier, T., Duarte-Hospital, C., Vignard, J., Boutet-Robinet, E., Sulyok, M., Snini, S. P., Alassane-Kpembi, I., Lippi, Y., Puel, S., Oswald, I. P., & Puel, O. (2020). Versicolorin A, a precursor in aflatoxins biosynthesis, is a food contaminant toxic for human intestinal cells. Environment International, 137, 105568. https://doi.org/10.1016/j.envint.2020.105568

Hasuda, A. L., Person, E., Khoshal, A. K., Bruel, S., Puel, S., Oswald, I. P., Bracarense, A. P. F. R. L., & Pinton, P. (2022). Deoxynivalenol induces apoptosis and inflammation in the liver: Analysis using precision-cut liver slices. Food and Chemical Toxicology, 163, 112930. https://doi.org/10.1016/j.fct.2022.112930

He, Y., Shi, Q., Ling, Y., Guo, H., Fei, Y., Wu, R., Tang, C., Zhang, X., & Yao, L. (2024). ABLIM1, a novel ubiquitin E3 ligase, promotes growth and metastasis of colorectal cancer through targeting IκBα ubiquitination and activating NF-κB signaling. Cell Death and Differentiation, 31(2), 203-216. https://doi.org/10.1038/s41418-024-01256-y

Hinze, C., & Boucrot, E. (2018). Endocytosis in proliferating, quiescent and terminally differentiated cells. Journal of Cell Science, 131(23), 1–10. https://doi.org/10.1242/jcs.216804

Hsu, C. M., Lin, P. M., Lin, H. C., Lai, C. C., Yang, C. H., Lin, S. F., & Yang, M. Y. (2016). Altered expression of imprinted genes in squamous cell carcinoma of the head and neck. Anticancer Research, 36(5), 2251–2258.

Huang, X., Zhao, L., & Peng, R. (2023). Hypoxia-Inducible Factor 1 and Mitochondria: An Intimate Connection. Biomolecules, 13(1), 1–14. https://doi.org/10.3390/biom13010050

Hussain, S. P., Schwank, J., Staib, F., Wang, X. W., & Harris, C. C. (2007). TP53 mutations and hepatocellular carcinoma: Insights into the etiology and pathogenesis of liver cancer. Oncogene, 26(15), 2166–2176. https://doi.org/10.1038/sj.onc.1210279

Janić Hajnal, E., Kos, J., Malachová, A., Steiner, D., Stranska, M., Krska, R., & Sulyok, M. (2020). Mycotoxins in maize harvested in Serbia in the period 2012–2015. Part 2: Non-regulated mycotoxins and other fungal metabolites. Food Chemistry, 317.https://doi.org/10.1016/j.foodchem.2020.126409

Jiang, M. P., Zheng, S. Y., Wang, H., Zhang, S. Y., Yao, D. S., Xie, C. F., & Liu, D. L. (2019). Predictive model of aflatoxin contamination risk associated with granary-stored corn with versicolorin A monitoring and logistic regression. Food Additives and Contaminants - Part A Chemistry, Analysis, Control, Exposure and Risk Assessment, 36(2), 308–319. https://doi.org/10.1080/19440049.2018.1562226

Kawai, K., Nozawa, Y., Maebayashi, Y., Yamazari, M., & Hamasaki, T. (1983). The Inhibition of Mitochondrial Respiration by Anthraquinone Mycotoxins, Averufin and Versicolorins A, B. 1983(18), 35–37. https://doi.org/https://doi.org/10.2520/myco1975.1983.18_35

Koen, E. J., & Collier, A. B. (2009). The basics of epithelial-mesenchymal transition. Physics of Plasmas, 119, 1420–1428. https://doi.org/10.1172/JCI39104.1420

Kozieł, M. J., Kowalska, K., & Piastowska-Ciesielska, A. W. (2021). Nrf2: a main responsive element in cells to mycotoxin-induced toxicity. Archives of Toxicology, 95(5), 1521–1533. https://doi.org/10.1007/s00204-021-02995-4

Kuleshov, M. V., Jones, M. R., Rouillard, A. D., Fernandez, N. F., Duan, Q., Wang, Z., Koplev, S., Jenkins, S. L., Jagodnik, K. M., Lachmann, A., McDermott, M. G., Monteiro, C. D., Gundersen, G. W., & Maayan, A. (2016). Enrichr: a comprehensive gene set enrichment analysis web server 2016 update. Nucleic Acids Research, 44(1), 90–97. https://doi.org/10.1093/nar/gkw377

Lee, J. G., Ahn, J. H., Kim, T. J., Lee, J. H., & Choi, J. H. (2015). Mutant p53 promotes ovarian cancer cell adhesion to mesothelial cells via integrin β4 and Akt signals. Scientific Reports, 5, 1–12. https://doi.org/10.1038/srep12642

Li, J., & Xu, Z. (2022). NR3C2 suppresses the proliferation, migration, invasion and angiogenesis of colon cancer cells by inhibiting the AKT/ERK signaling pathway. Molecular Medicine Reports, 25(4), 1–8. https://doi.org/10.3892/mmr.2022.12649

Li, Y., Huang, J., Zhao, Y. L., He, J., Wang, W., Davies, K. E., Nosé, V., & Xiao, S. (2007). UTRN on chromosome 6q24 is mutated in multiple tumors. Oncogene, 26(42), 6220–6228. https://doi.org/10.1038/sj.onc.1210432

Liang, Y., Wang, B., Chen, S., Ye, Z., Chai, X., Li, R., Li, X., Kong, G., Li, Y., Zhang, X., Che, Z., Xie, Q., Lian, J., Lin, B., Zhang, X., Huang, X., Huang, W., Qiu, X., & Zeng, J. (2021). Beta-1 syntrophin (SNTB1) regulates colorectal cancer progression and stemness via regulation of the Wnt/β-catenin signaling pathway. Annals of Translational Medicine, 9(12), 1016. https://doi.org/10.21037/atm-21-2700

Lippi, Y., & Soubès, F. (2023). MATRiX: a shiny application for Mining and functional Analysis of TRanscriptomics data. swh:1:dir:a78cb8f1c0fca114d6fc7fcdcf6659545570da1b⟩. ⟨hal-04251787⟩

Lu, C., Yang, Z., Yu, D., Lin, J., & Cai, W. (2020). RUNX1 regulates TGF-β induced migration and EMT in colorectal cancer. Pathology Research and Practice, 216(11), 153142. https://doi.org/10.1016/j.prp.2020.153142

Luo, Shen, & Levine, R. L. (2009). Methionine in proteins defends against oxidative stress. The FASEB Journal, 23(2), 464–472. https://doi.org/10.1096/fj.08-118414

Luo, Su, Terciolo, C., Neves, M., Puel, S., Naylies, C., Lippi, Y., Pinton, P., & Oswald, I. P. (2021). Comparative sensitivity of proliferative and differentiated intestinal epithelial cells to the food contaminant, deoxynivalenol. Environmental Pollution, 277, 116818. https://doi.org/10.1016/j.envpol.2021.116818

584 Marrone, A. K., Tryndyak, V., Beland, F. A., & Pogribny, I. P. (2016). MicroRNA responses
585 to the genotoxic carcinogens aflatoxin B1 and benzo[a]pyrene in human HepaRG cells.
586 Toxicological Sciences, 149(2), 496–502. https://doi.org/10.1093/toxsci/kfv253

587 Meek, D. W., & Anderson, C. W. (2009). Posttranslational modification of p53: cooperative
588 integrators of function. Cold Spring Harbor Perspectives in Biology, 1(6), 1–16.
589 https://doi.org/10.1101/cshperspect.a000950

590 Morikawa, M., Derynck, R., & Miyazono, K. (2016). TGF-b and the TGF-b Family: Context-
591 Dependent Roles in Cell and Tissue Physiology. Cold Spring Harbor Perspectives in Biology,
592 8, 1–24. https://doi.org/10.1101/cshperspect.a021873

593 Muto, Y., Matsunami, M., Kawai, K., & Hamasaki, T. (1997). The effect of versicolorin A on
594 electrical conductance in planar lipid bilayer membranes. Mycotoxins, 1997(44), 45–48.
595 https://doi.org/10.2520/myco1975.1997.45

596 Nossol, C., Barta-böszörményi, A., Kahlert, S., & Zuschratter, W. (2015). Comparing Two
597 Intestinal Porcine Epithelial Cell Lines (IPECs): Morphological Differentiation , Function and
598 Metabolism. PLoS ONE, 10(7), 1–20. https://doi.org/10.1371/journal.pone.0132323

599 Payros, D., Garofalo, M., Pierron, A., Soler-Vasco, L., Al-Ayoubi, C., Maruo, V. M., Alassane-
600 Kpembi, I., Pinton, P., & Oswald, I. P. (2021). Mycotoxins in human food: A challenge for
601 research. Cah. Nutr. Diet, 56, 170–183.
602 https://doi.org/https://doi.org/10.1016/j.cnd.2021.02.001

603 Pierron, A., Neves, M., Puel, S., Lippi, Y., Soler, L., Miller, J. D., & Oswald, I. P. (2022).
604 Intestinal toxicity of the new type A trichothecenes, NX and 3ANX. Chemosphere, 288(P1),
605 132415. https://doi.org/10.1016/j.chemosphere.2021.132415

606 Pinton, P., Braicu, C., Nougayrede, J. P., Laffitte, J., Taranu, I., & Oswald, I. P. (2010).
607 Deoxynivalenol impairs porcine intestinal barrier function and decreases the protein expression
608 of claudin-4 through a mitogen-activated protein kinase-dependent mechanism. Journal of
609 Nutrition, 140(11), 1956–1962. https://doi.org/10.3945/jn.110.123919

610 R Core Team. (2018). A Language and Environment for Statistical Computing. R Foundation
611 for Statistical Computing, Vienna.

612 Ren, Z., He, H., Zuo, Z., Xu, Z., Wei, Z., & Deng, J. (2019). The role of different SIRT1-
613 mediated signaling pathways in toxic injury. Cellular and Molecular Biology Letters, 24(1), 1–
614 10. https://doi.org/10.1186/s11658-019-0158-9

615 Riley, T., Sontag, E., Chen, P., & Levine, A. (2008). Transcriptional control of human p53-
616 regulated genes. Nature Reviews Molecular Cell Biology, 9(5), 402–412.
617 https://doi.org/10.1038/nrm2395

618 Ritchie, M. E., Phipson, B., Wu, D., Hu, Y., Law, C. W., Shi, W., & Smyth, G. K. (2015).
619 Limma powers differential expression analyses for RNA-sequencing and microarray studies.
620 Nucleic Acids Research, 43(7), e47. https://doi.org/10.1093/nar/gkv007

621 Schrenk, D., Bignami, M., Bodin, L., Chipman, J. K., del Mazo, J., Grasl-Kraupp, B.,
622 Hogstrand, C., Hoogenboom, L., Leblanc, J. C., Nebbia, C. S., Nielsen, E., Ntzani, E., Petersen,
623 A., Sand, S., Schwerdtle, T., Vleminckx, C., Marko, D., Oswald, I. P., Piersma, A., … Wallace,

H. (2020). Scientific opinion – Risk assessment of aflatoxins in food. EFSA Journal, 18(3), 112. https://doi.org/10.2903/j.efsa.2020.6040

Smela, M. E., Currier, S. S., Bailey, E. A., & Essigmann, J. M. (2001). The chemistry and biology of aflatoxin B1: from mutational spectrometry to carcinogenesis. Carcinogenesis, 22(4), 535–545. https://doi.org/10.1093/carcin/22.4.535

Soler, L., Stella, A., Seva, J., Pallarés, F. J., Lahjouji, T., Burlet-Schiltz, O., & Oswald, I. P. (2020). Proteome changes induced by a short, non-cytotoxic exposure to the mycoestrogen zearalenone in the pig intestine. Journal of Proteomics, 224, 103842. https://doi.org/10.1016/j.jprot.2020.103842

Stewart-Ornstein, J., & Lahav, G. (2017). P53 dynamics in response to DNA damage vary across cell lines and are shaped by efficiency of DNA repair and activity of the kinase ATM. Science Signaling, 10(476). https://doi.org/10.1126/scisignal.aah6671

Tang, B. L. (2016). Sirt1 and the mitochondria. Molecules and Cells, 39(2), 87–95. https://doi.org/10.14348/molcells.2016.2318

Theumer, M. G., Henneb, Y., Khoury, L., Snini, S. P., Tadrist, S., Canlet, C., Puel, O., Oswald, I. P., & Audebert, M. (2018). Genotoxicity of aflatoxins and their precursors in human cells. Toxicology Letters, 287, 100–107. https://doi.org/10.1016/j.toxlet.2018.02.007

West, A. P., Khoury-hanold, W., Staron, M., Tal, M. C., Cristiana, M., Lang, S. M., Bestwick, M., Duguay, B. A., Raimundo, N., Macduff, D. A., Kaech, S. M., Smiley, J. R., Means, R. E., & Shadel, G. S. (2015). Mitochondrial DNA Stress Primes the Antiviral Innate Immune Response. Nature, 520(7548), 553–557. https://doi.org/10.1038/nature14156.

Xie, Z., Bailey, A., Kuleshov, M. V., Clarke, D. J. B., Evangelista, J. E., Jenkins, S. L., Lachmann, A., Wojciechowicz, M. L., Kropiwnicki, E., Jagodnik, K. M., Jeon, M., & Ma'ayan, A. (2021). Gene Set Knowledge Discovery with Enrichr. Current Protocols, 1(3), 1–84. https://doi.org/10.1002/cpz1.90

Yang, X., Liu, F., Xu, Z., Chen, C., Li, G., Wu, X., & Li, J. (2004). Growth hormone receptor expression in human colorectal cancer. Digestive Diseases and Sciences, 49(3), 1493–1498. https://doi.org/10.1023/B:DDAS.0000042254.35986.57

Zhang, T., & Kraus, W. L. (2010). SIRT1-dependent Regulation of Chromatin and Transcription: Linking NAD+ Functions. Biochim Biophys Acta, 1804(8), 1666–1675. https://doi.org/10.1016/j.bbapap.2009.10.022

Zhu, Y.-H., Li, J.-B., Wu, R.-Y., Yu, Y., Li, X., Li, Z.-L., Zhang, H.-L., Feng, G.-K., Deng, R., & Zhu, X.-F. (2020). Clinical significance and function of RDH16 as a tumor-suppressing gene in hepatocellular carcinoma. Hepathology Research, 50, 110–120. https://doi.org/10.1111/hepr.13432

Figures:

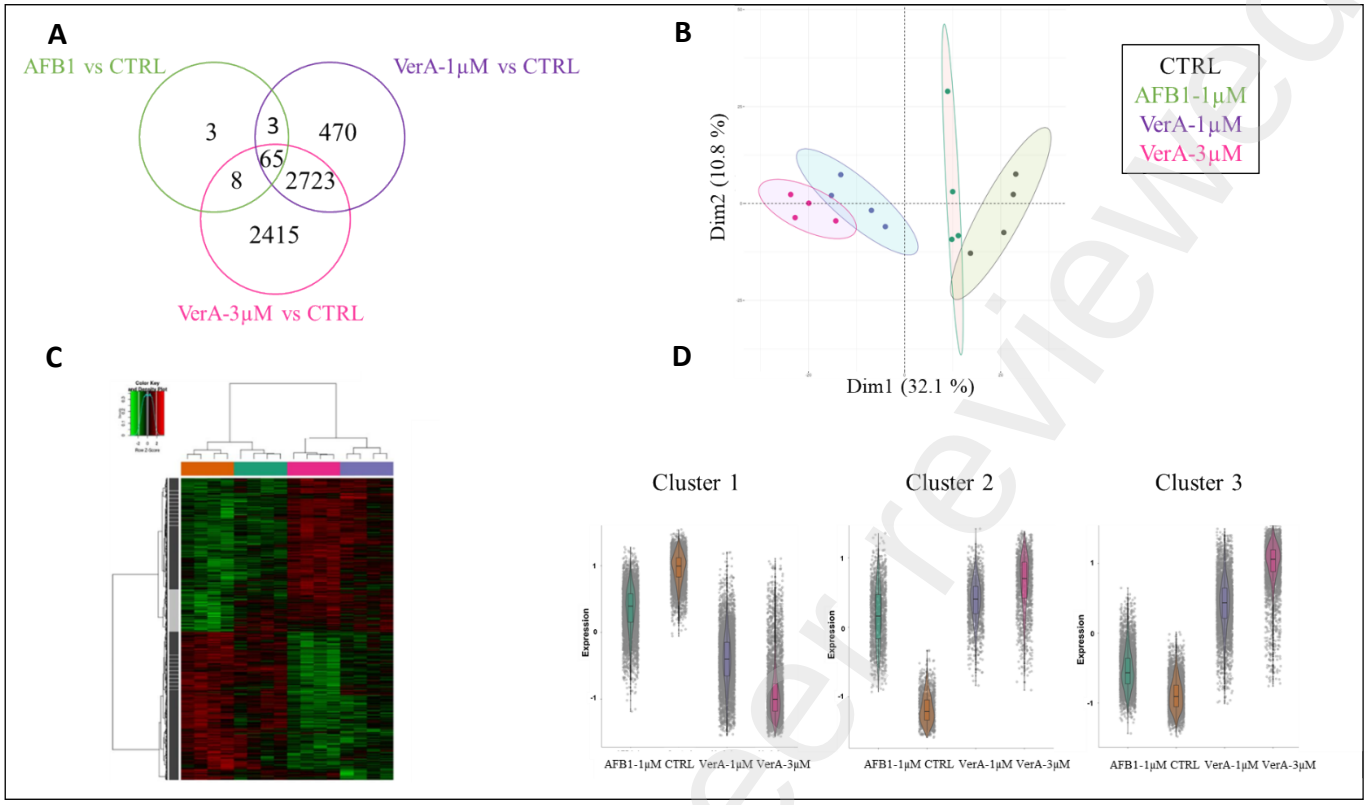

Figure 1. Gene expression profile of intestinal cells exposed to AFB1 (1 µM), VerA (1 µM), VerA (3 µM)

(A) *Venn diagram representing the differentially expressed genes (Adjusted p-value < 0.05) in cells exposed to 1 µM AFB1 (in green), 1 µM VerA (in purple) and 3 µM VerA (in pink) compared to solvent control cells.* ***(B)*** *Principal component analysis of normalized expression signals on all samples:1 µM AFB1 (green), 1 µM VerA (purple) and 3 µM VerA (pink) and solvent control DMSO (black).* ***(C)*** *Heat map representing differentially expressed genes exposed to AFB1 (1 µM), VerA (1 µM), VerA (3 µM) compared to control (DMSO, adjusted p-value < 0.05). Individual gene expression is represented in the heatmap, and the hierarchical clustering was obtained from individual expression values using Pearson correlation coefficient as distance and Ward's criterion for agglomeration. Red and green indicate values above and below the mean averaged centred and scaled expression values (Z-score), respectively. Black indicates values close to the mean. According to the probe clustering (left panel), 3 gene clusters showed specific gene expression profiles.* ***(D)*** *Violin plots with strip charts representing expression profiles of the three clusters identified by the clustering of differentially expressed probes illustrated in the heat map in (C). The average expression signal (z-score) of the probes is plotted for each of the four conditions: 1 µM AFB1 (green), 1 µM VerA (purple) and 3 µM VerA (pink) and solvent control DMSO (orange) cells.*

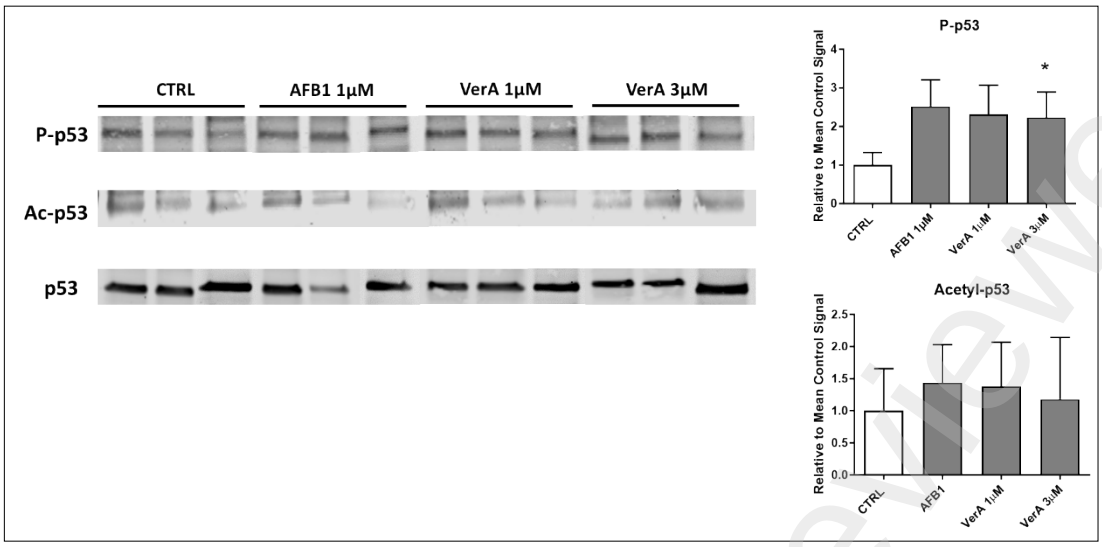

Figure 2. Immunoblotting analysis of phospho-p53 and acetyl-p53 in intestinal cells exposed to AFB1 (1 µM), VerA (1 µM), VerA (3 µM) or not (CTRL). *(A) Representative blots of 3 paired samples of phospho-p53, acetyl-p53 and p53* ***(B)*** *Relative quantification of normalized signal (arbitrary units). Values of phospho-p53 and acetyl-p53 are relative to those of p53. Values are means with standard errors of the mean of the control represented by vertical bars (n = 3). Asterisks indicate statistical differences (*p < 0 .05).*

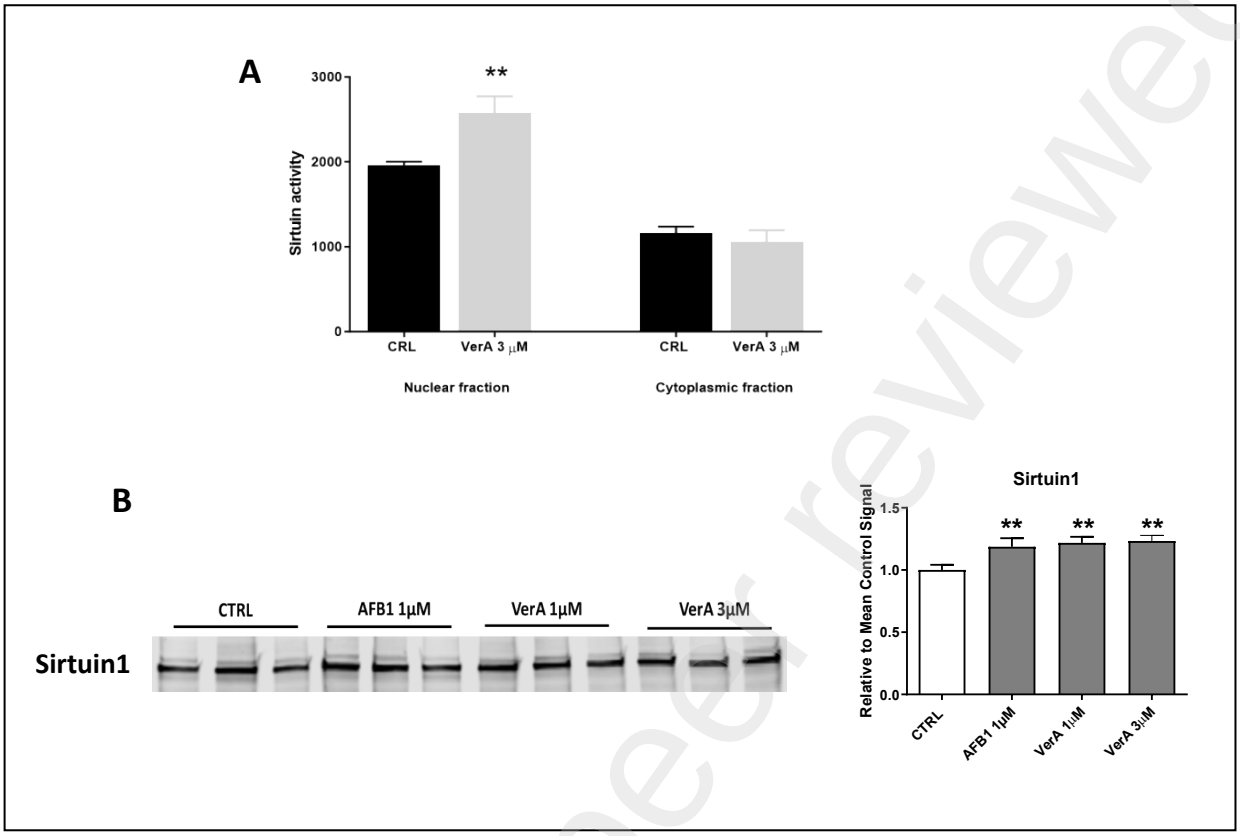

Figure 3. Effects of VerA on the sirtuin signaling pathway in intestinal cells. (A) *Deacetylase activity of sirtuins in subcellular fractions of intestinal cells exposed to 3 μM VerA for 6 h. Values are means with standard errors of the mean represented by vertical bars (n = 3). Asterisks indicate a significant difference (**p < 0.01).* ***(B)*** *Immunoblotting analysis of sirtuin 1 in intestinal cells exposed to AFB1 (1 μM), VerA (1 μM), VerA (3 μM) or not (CTRL). (B, Left) Representative blots of 3 paired samples of sirtuin 1 (B, Right) Relative quantification of normalized signal (arbitrary units). Values are means with standard errors of the mean of the control represented by vertical bars (n = 3). Asterisks indicate statistical differences (**p < 0 .01).*

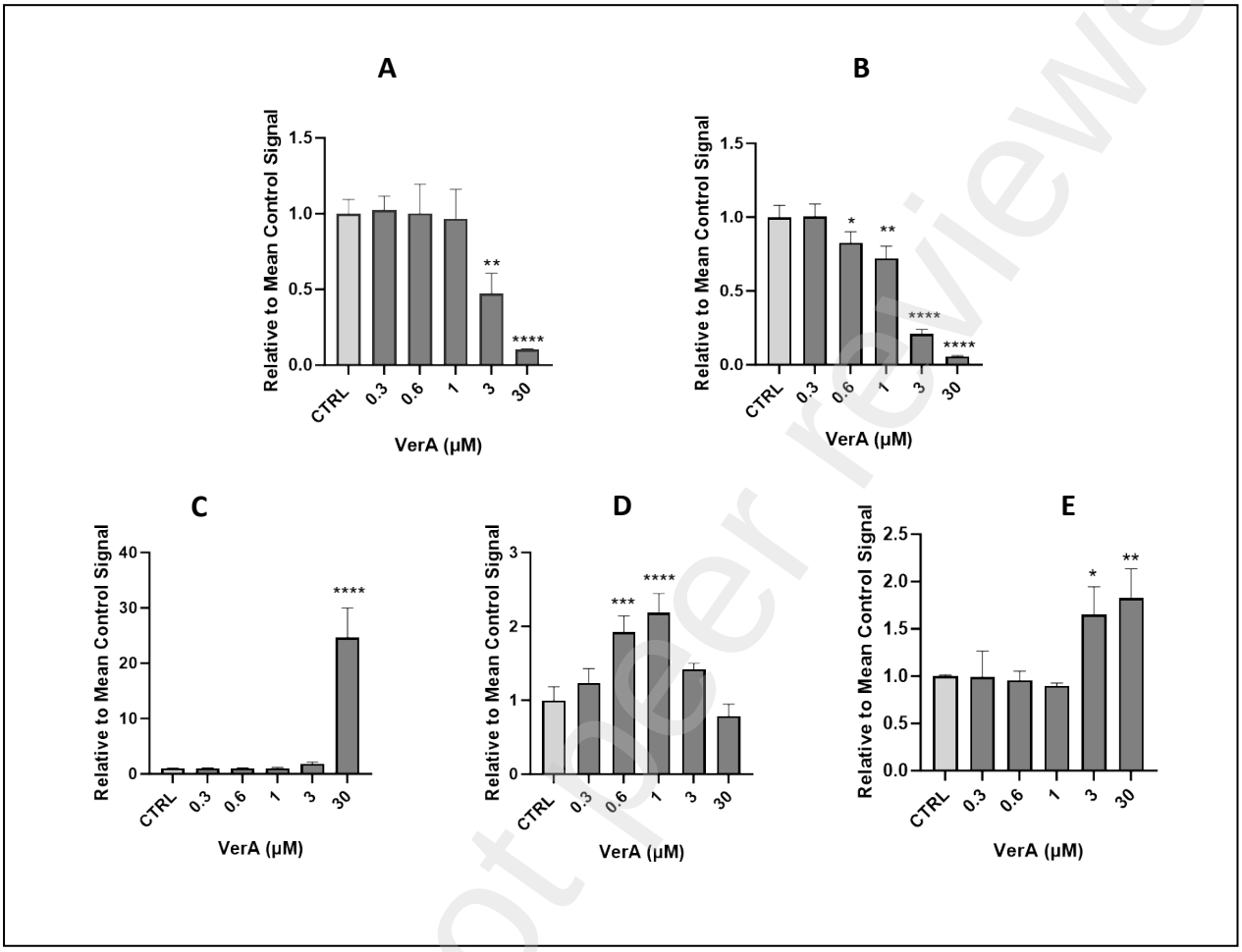

Figure 4. Evaluation of the mitochondrial toxicity of VerA in intestinal cells*. Measurement of ATP levels in intestinal cells exposed to different doses of VerA for 6 h* ***(A)*** *in the presence of glucose or* ***(B)*** *in the presence of galactose. Evaluation of* ***(C)*** *cytotoxicity,* ***(D)*** *caspase 3/7 activation and* ***(E)*** *mitochondrial superoxide levels. Values are means with standard errors relative to the mean of the control (n = 3). Asterisks indicate statistical differences (*p < .05; **p < .01, ***p < .001, ****p < .0001).*

Tables:

Table 1. Differentially expressed genes in cluster 1 associated with the GO molecular function "RNA binding" in intestinal cells exposed to AFB1 (1 µM) and VerA (1 µM / 3 µM) compared to solvent control DMSO. Adjusted P.Values < 0.05 are highlighted in grey.

Gene name	Genes associated with the GO RNA binding molecular function						Function
	adj.P.Val			Fold Change vs. Control			
	VerA 1 µM	VerA 3 µM	AFB1 1 µM	VerA 1 µM	VerA 3 µM	AFB1 1 µM	
Down-regulated genes							
SRPK1	4.1E-03	9.1E-06	0.27	0.69	0.47	0.83	Regulation of constitutive and alternative splicing
EIF4G1	0.67	6.2E-03	0.54	0.96	0.8	0.92	Essential for transcription
DHX9	3.7E-02	0.14	0.2	0.77	0.85	0.79	Involved in DNA replication, transcriptional activation, post-transcriptional RNA regulation, mRNA translation and RNA-mediated gene silencing
NME1	3.6E-02	9.7E-03	0.59	0.85	0.83	0.93	Involved in cell proliferation, differentiation and development, signal transduction, G protein-coupled receptor endocytosis, and gene expression.
EIF4G2	0.12	1.2E-02	0.96	0.81	0.71	0.98	General repressor of translation by forming translationally inactive complexes
TSR1	2.4E-02	3.5E-04	0.95	0.82	0.65	0.98	Involved in endonucleolytic cleavage of tricistronic rRNA transcript and maturation of SSU-rRNA from tricistronic rRNA transcript
NOP56	5.3E-04	4.0E-08	0.95	0.78	0.57	0.99	Core component of box C/D small nucleolar ribonucleoprotein (snoRNP) particles
RAN	0.46	4.1E-04	0.99	0.95	0.79	1.00	Favors translocation of RNA and proteins through the nuclear pore complex. Involved in control of DNA synthesis and cell cycle progression
BMS1	8.8E-03	2.6E-05	0.81	0.87	0.77	0.97	Processing of Capped Intron-Containing Pre-mRNA
NOP14	1.3E-02	8.8E-05	0.65	0.84	0.74	0.94	Nucleolar processing of pre-18S ribosomal RNA

GTPBP4	1.5E-03	1.7E-06	0.84	0.84	0.75	0.98	Involved in the biogenesis of the 60S ribosomal subunit
Up-regulated genes							
TOP1	9.0E-03	1.3E-04	0.71	1.15	1.22	1.05	Controls and alters the topologic states of DNA during transcription
TOP2B	8.9E-02	4.4E-04	0.86	1.10	1.20	1.03	Controls and alters the topologic states of DNA during transcription

Table 2. Differentially expressed genes from the Nrf2/ARE signaling pathway in intestinal cells exposed to AFB1 (1 µM) and VerA (1 µM / 3 µM) compared to solvent control DMSO. Adjusted P.Values < 0.05 are highlighted in grey.

Gene name	Genes involved in Nrf2/ARE response					
	adj.P.Val			Fold Change vs. Control		
	VerA 1 µM	VerA 3 µM	AFB1 1 µM	VerA 1 µM	VerA 3 µM	AFB1 1 µM
NFE2L2	0.10	0.42	0.33	1.17	1.08	1.15
KEAP1	0.99	0.94	0.97	1.00	0.99	1.01
CAT	3.73E-03	1.02E-03	0.52	1.27	1.29	1.10
GSS	0.76	0.55	0.90	0.96	0.94	0.96
SOD1	0.52	0.18	0.10	1.04	1.07	1.00
SOD2	0.13E-02	1.52E-04	0.15	0.74	0.72	0.83
GPX1	0.98	0.42	0.96	1.00	1.04	0.99
GPX1	0.15	2.81E-02	0.93	1.07	1.09	1.01
GPX2	3.33E-04	2.99E-06	2.74E-02	0.76	0.70	0.77
GPX3	3.13E-02	0.32	0.53	0.84	0.92	0.91
GPX4	0.69	0.27	0.82	1.02	1.05	0.97
GPX6	0.62	0.19	0.92	0.94	0.87	1.04
GPX8	7.99E-02	4.65E-03	0.95	1.12	1.19	1.01
NQO1	7.93E-06	3.97E-05	0.79	1.34	1.27	0.96
HMXO1	0.50	3.61E-03	0.47	0.95	0.86	0.93
GCLC	0.32	2.5	0.79	0.91	0.84	0.94
GCLM	0.63E-04	4.95E-06	0.82	1.19	1.32	1.03
TXN	0.135	5.99E-03	0.92	0.92	0.87	0.98